

Einstein Telescope WG1 Report

Selection criteria for ET candidate sites

M.G. Beker¹, R. DeSalvo², M. Doets¹, Steven Dorsher³,
E. Hennes¹, H. Grote⁴, J. Harms³, K. Kuroda⁵, V. Mandic³,
D.S. Rabeling^{1,6}, J.F.J. van den Brand^{1,6} (contact person), C.M. van Leeuwen⁶

¹ *Nikhef, P.O. Box 41882, Amsterdam, the Netherlands*

² *California Institute of Technology, East Bridge, Pasadena, California 91125, USA*

³ *University of Minnesota, 116 Church Street SE, Minneapolis, MN 55455, USA*

⁴ *Institut für Gravitationsphysik, Leibniz Universität Hannover and
Max-Planck-Institut für Gravitationsphysik (Albert-Einstein-Institut),
Callinstrasse 38, D-30167 Hannover, Germany*

⁵ *Institute for Cosmic Ray Research, University of Tokyo, Kashiwa, Chiba 277-8582, Japan*

⁶ *VU University Amsterdam, 1081 HV de Boelelaan, Amsterdam, the Netherlands*

November 22, 2009

Abstract

Seismic noise plays a dominant role in limiting the design sensitivity of third-generation gravitational wave detectors at very low frequencies (1 - 10 Hz). This study addresses the selection criteria for candidate sites for Einstein Telescope that should result in relatively low seismic and gravity gradient noise.

Contents

1	Introduction	3
2	Ambient ground motion	4
2.1	Slow ground motion in hard rock	4
2.2	Slow ground motion in salt mines	5
2.3	Seismic motion	7
2.3.1	Microseismic noise	9
2.3.2	Cultural noise	11
2.3.3	Wind noise	14
2.4	Geological and geographic dependence	15
3	Specific sites	18
3.1	CLIO site at Kamioka, Japan	18
3.2	Homestake (Dusel) site at Black Hills, South Dakota, USA	19
3.3	Sites in Germany	21
3.4	Experience from particle accelerator sites	22
4	Site requirements from logistical arguments	23
5	Summary	24

1 Introduction

The noise sources that limit the design sensitivity of the first and second generation gravitational wave detectors are well identified. As an example, in Fig. 1 the design sensitivity of an advanced detector (2nd generation) is reported [1] listing the main noise sources. The figure also shows the design sensitivity of Einstein Telescope. At very low frequency the seismic noise plays a

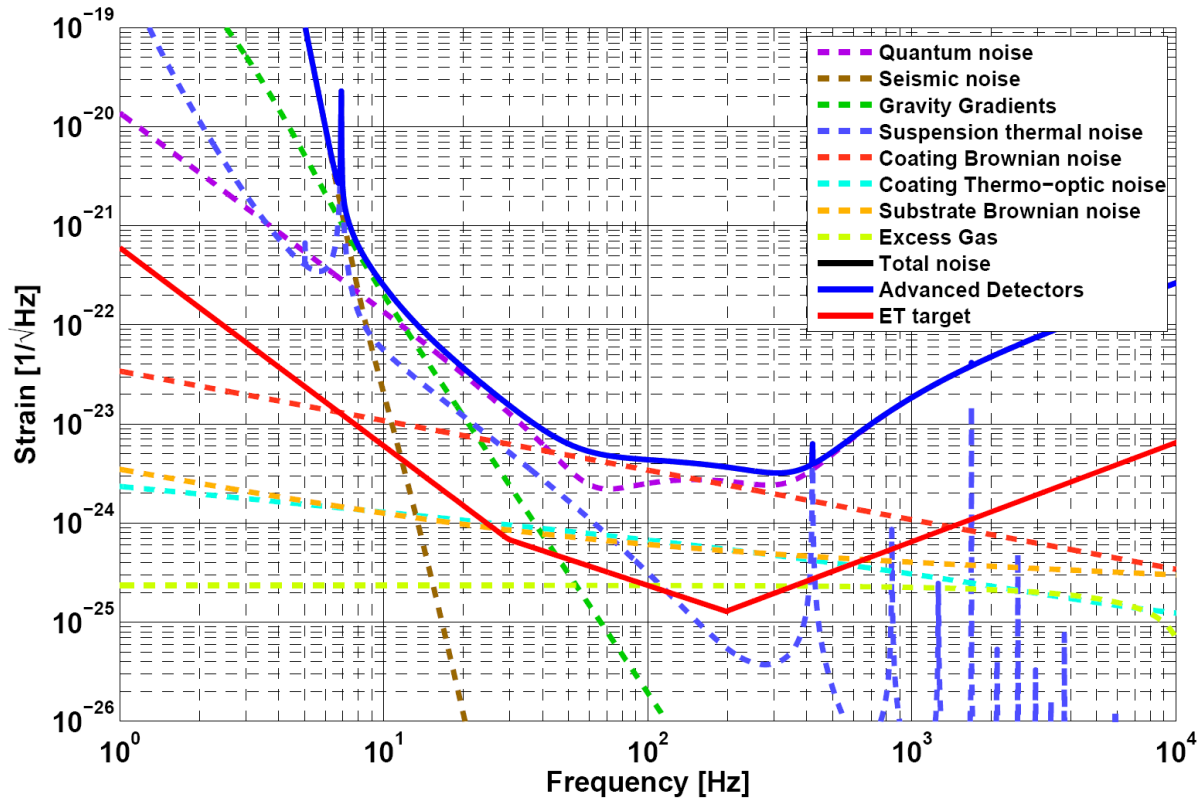


Figure 1: Noise contributions [1] to the sensitivity of a potential advanced detector (blue solid curve). The solid red curve is an approximation of the design target for the sensitivity of Einstein Telescope. It is seen that in the frequency range 1 - 10 Hz seismic and gravity gradient noise dominate.

dominant role. The seismic filter chain used to suspend the main optics of the interferometer must be designed carefully to prevent seismic induced vibrations to pass through and affect the detector sensitivity. More importantly, the vibrating soil can directly couple to the suspended masses (so called Newtonian noise (NN) or gravity gradient noise (GGN)). Furthermore, seismic noise complicates the control of the seismic filter chain (giving rise to the so-called control noise).

The required reduction of the influence of seismic noise with respect to the second generation detectors can be achieved through an improvement of the vibration isolation of the mirrors (also termed test masses) and of the controllability of the suspension. To suppress the influence of seismic displacement noise, the test masses will be suspended from sizable and complex attenuation chains. Nevertheless, fluctuating gravitational fields directly couple to the test masses themselves, bypassing all previous attenuation stages. The time-varying contributions to the gravity gradient noise originate from both seismic and atmospheric density fluctuation, generating a stochastic gravitational force on the test mass. In general, seismic waves originate from human induced activities (cultural seismic noise), ocean and ground water dynamics, slow gravity

drifts, and atmospheric influences. Since no general filter or shield can be built for gravitational coupling it is imperative that sites with relatively low seismicity should be identified. This is the main activity of work package 1 of the Einstein Telescope design study: the definition of site requirements and the proposition of the possible sites in Europe, having satisfactory specifications. The need to reduce both the seismic and gravity gradient noise seems to be fulfilled by an underground site. Low seismic activity and uniformity of the soil plays a dominant role in the site identification process since they may facilitate GGN subtraction schemes.

This report is structured as follows: ambient ground motion is addressed in section 2. First, slow ground motion in hard rock and salt is discussed. This is followed by a discussion of seismic motion that addresses microseisms, cultural and wind noise. The section concluded with outlining the dependence of ambient noise on geography and geology. Section 3 present information on specific sites: Kamioka (Japan), Homestake (USA), Germany and particle accelerator sites. The report is completed with section 4 that presents a discussion on logistical aspects.

2 Ambient ground motion

Interferometric gravitational wave detectors are large and complex and the selection of their site is an issue of great importance. Ideally, the site should feature minimal seismic cultural noise (now and in the future) and gravity gradient noise, while proximity to an existing laboratory would be an advantage. Most of the seismic cultural noise propagates over the surface, and attenuates with depth. Similarly, gravity gradient noise from surface waves decreases with depth, in part due to geometric cancellation effects. Moreover, the expected higher coherence of the waves may lead to more effective gravity gradient subtraction schemes. Consequently, the ideal site may be located underground at sufficient depth.

Presently, the large interferometric detectors GEO600, LIGO, TAMA and VIRGO are placed on the surface of the earth and, consequently, are more sensitive to seismic disturbances. In fact, their operation is limited by seismic displacement noise and their sensitivity rapidly deteriorates for frequencies below about 10 Hz (see also Fig. 1). At these low frequencies Virgo has realized good performance due to a suitable attenuation scheme. From a mathematical point of view ground motion is a random process and can be represented by a power spectrum. At a moderately quiet site on or just below the surface of the earth, seismic motion in all three dimensions follows a spectrum of approximately $100 \text{ nm}/f^2\sqrt{\text{Hz}}$ for frequencies f above about 1 Hz. For third-generation gravitational wave detectors the goal is to identify sites with seismic noise of about $1 \text{ nm}/f^2\sqrt{\text{Hz}}$ for frequencies above 1 Hz.

2.1 Slow ground motion in hard rock

The position of test masses will experience diffusive ground movement and perform Brownian motion characterized by the variance of the relative displacement which scales as a product of temporal and spatial intervals. This residual diffusive motion can be approximated by ‘the ATL law’ [2, 3]. This empirical rule states that the rms relative displacement dx of two points located at a distance L grows with time T according to

$$\langle dx^2 \rangle = ATL, \tag{1}$$

where A is a constant of the order $10^{-5\pm 1} \mu\text{m}^2/(s \cdot m)$ that depends on the site. The diffusion wandering takes place in all directions. Fig. 2 shows alignment data of LEP at CERN. It is seen

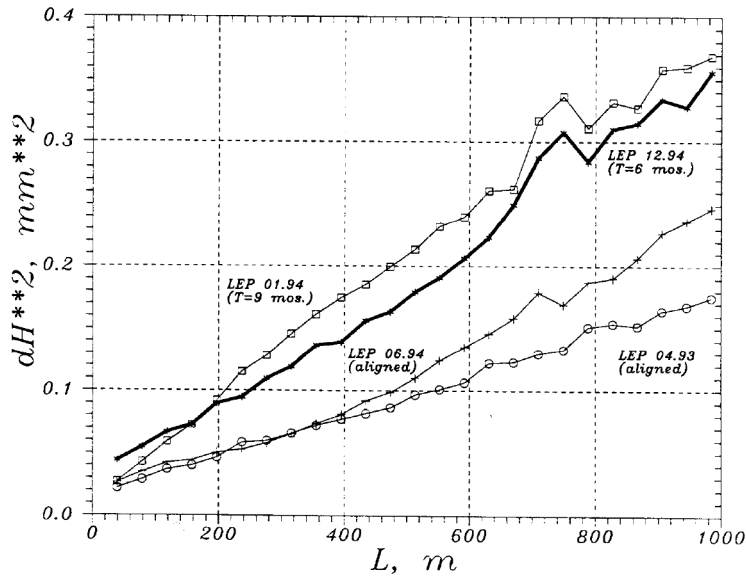


Figure 2: Mean squared height differences $dH^2(L) = \langle (H(l+L) - H(l))^2 \rangle$ for LEP at CERN versus distance L [4]. Note that LEP was aligned on 04.1993. Data labeled 01.1994 were collected 9 months later; LEP was again aligned on 06.1994 and 12.1994 corresponds to data obtained 6 months later.

that the larger the distance L between the tunnel pieces, the larger the variance of their relative displacement in time. Fig. 3 shows the variance of relative displacements divided by observation time versus the distance between points for SPS, PEP, UNK and SLAC (data from [5]). A fit gives $A = (1.0 \pm 0.5) \times 10^{-4} \mu m^2 / (m \cdot s)$. For two test masses separated at 10 km this results in a drift of $\sqrt{\langle \delta x^2 \rangle} \approx 6$ mm over a time period of 1 year. Similar values have been obtained for the rms orbit drifts versus time for LHC (an estimated rms closed-orbit distortion of 5.7 mm over 1 year).

The diffusion parameter A has been studied as function of depth, and the following empirical expression has been obtained,

$$A [\mu m^2 / (s \cdot m)] = \frac{3}{1 + H^{3/4}}, \quad (2)$$

with depth H in meters. It follows that the variance of relative displacements $\sqrt{\langle \delta x^2 \rangle}$ decreases in hard rock by about an order of magnitude at a depth of 400 m compared to the corresponding surface value.

2.2 Slow ground motion in salt mines

Various salt deposits can be found in Europe that were formed as evaporites (a type of sedimentary rock). Fig. 4 shows their distribution in northern Europe. Rock salt has been mined at various places in Europe, with some structures now in use as deep geological repositories for nuclear waste. Sites as Schacht Asse II, Morsleben, and Gorleben (planned) store waste at a depth of about 750 m. Salt has various attractive features for realizing underground constructions, such as relatively low-cost mining without need for armoring columns and struts. However, salt is also known for its plasticity effects. For example, the Institut für Gebirgsmechanik in Leipzig

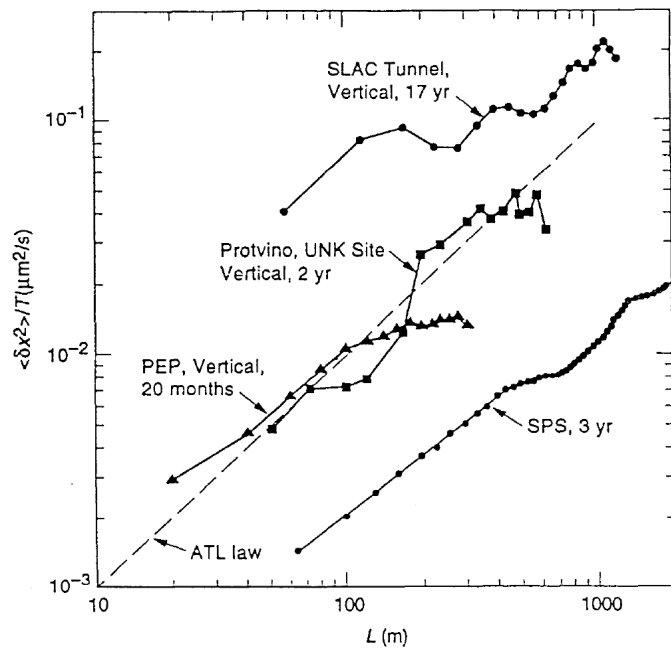


Figure 3: Variance of relative displacements divided by observation time versus the distance between points for SPS, PEP, UNK and SLAC (data from [5]).

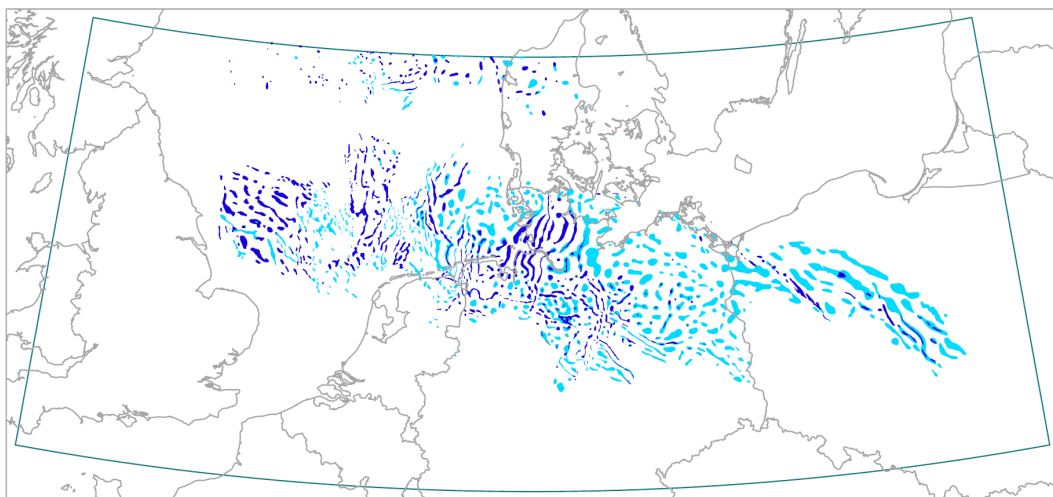


Figure 4: Geological map of salt structures in northern Europe (data from BGR Germany [6]).

monitors salt motion in Asse II. Presently, the capping mass in Asse II moves 15 cm per year. It is predicted [16] that from the beginning of 2014, an increase in the loss of the load carrying capacity due to plasticity effects in the salt dome will result in an increased displacement of the capping mass. This may lead to an uncontrollable increase in water inflow in that mine and make the continued operation as a dry pit impossible. Elsewhere and in most salt structures, water inflow is not expected to be the main issue. Instead rock creep should be considered as it both misaligns the structures and generates creep noise, where the latter may be of fractal origin.

2.3 Seismic motion

Noise studies [17, 18, 19, 20] differentiate noise sources according to frequency. Noise at frequencies below about 1 Hz is termed ‘microseismic’. Its sources are dominantly natural (*i.e.* non cultural and non-local) and depend on oceanic and large-scale meteorological conditions (*e.g.* monsoons and cyclones). Around 1 Hz wind effects and local meteorological conditions show up, while for frequencies above 1 Hz, additional sources (besides natural) are related mainly to human activity. Such noise is termed ‘cultural noise’ or ‘microtremors’. It should be noted that the 1 Hz division is not absolute.

Peterson [7] generated noise power spectral density plots for frequencies up to 10 Hz for 75 seismic stations distributed worldwide (see Fig. 5). Several years of data were collected (about

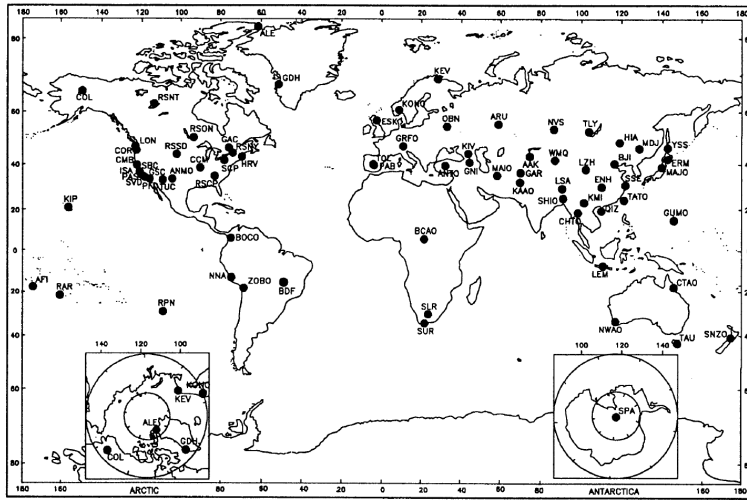


Figure 5: Map showing the approximate locations of the stations used in the definition of the Peterson (1993) seismic background noise models [7].

12,000 spectra). From a combined fit to data from both surface and borehole sensors (100 - 340 m depth) he derived a new low noise model (NLNM) that replaced his earlier low noise model [8]. The data and fit are shown in Fig. 6. Note that also a new high noise model was derived, but its implications will not be discussed here. The power spectral density (PSD)¹ is expressed in decibels ($10 \times \text{Log}(\text{m}^2/(\text{s}^4\text{Hz}))$) and refers to a squared acceleration of $1 (\text{m}/\text{s}^2)^2/\text{Hz}$. The largest PSD values are seen at long periods. The surface of the Earth experiences large external

¹In the literature various representations are used, such as the root power spectral density (RPSD), acceleration, velocity and displacement densities. The conversions are straightforward and in the following we will freely use various representations.

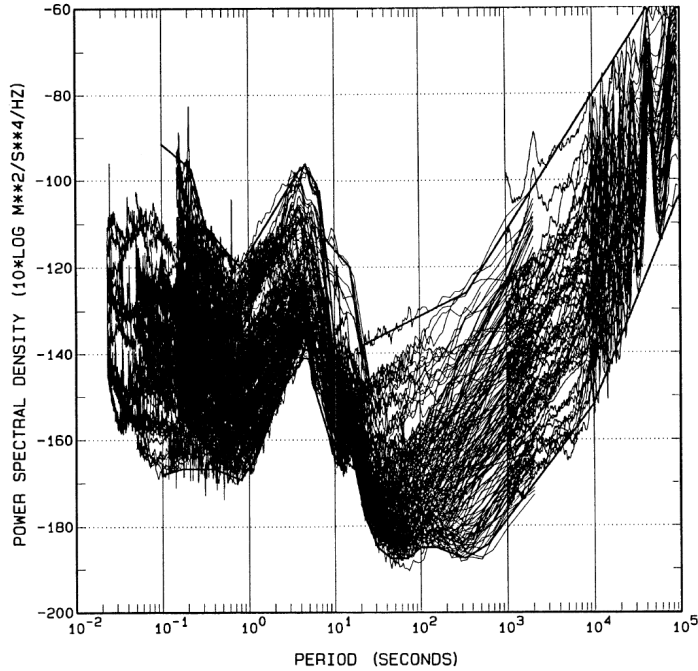


Figure 6: Overlay of network station spectra used in Peterson’s background noise study [7] together with straight-line segments fitted to the high-noise and low-noise envelopes of the overlay.

forces due to the gravitational attractions of the Moon and Sun. This causes for example the surface of the Earth to rise and fall with amplitudes of about 0.5 m with respect to the center of the Earth. This tidal motion can be seen in Fig. 6 at a period of 4.3×10^4 s. Since the motion occurs at very low frequency the test masses will move *coherently* and differential motion presents no problem. Large PSD values are observed at periods clustered around 5 and 18 s which correspond to microseisms. Note that a large dynamic range of more than four orders of magnitude (90 dB) is needed to accommodate signals between 1 and 100 s.

For Einstein Telescope the critical frequencies f are in the range 1 - 10 Hz, where the response is most variable mainly due to cultural noise. It is therefore important to choose a site location far from human activities both at present and in future. The NLNM yields a PSD of -168.6 dB/Hz at 1 Hz and this corresponds to acceleration density of $0.37 \text{ ng}/\sqrt{\text{Hz}}$. The NLNM predicts an approximately flat PSD response for accelerations in the frequency band of 1 - 10 Hz (the domelike structure observed at 3 Hz in Fig. 5 is believed to be due to instrumental effects, notably the STS sensor gain). Corresponding displacements can be found by double integration of the accelerations yielding the typical $1/\omega^2$ angular frequency dependence. The conversion should take the integration bandwidth into account (often 1/3 octave is used corresponding to a range of $\pm 10\%$ about the center value). Note that when a Gaussian signal is passed through a narrow-band filter, the absolute peak signals of the filtered signal envelope will have a Rayleigh distribution (yielding a factor 1.253σ for $|\bar{x}_P|$). Lowest possible displacements according to the NLNM are about $0.1 \text{ nm}/\sqrt{\text{Hz}}$ at 1 Hz and decrease with f^{-2} .

It has been pointed out [9] that many of the stations used by Peterson are now encroached upon by urban areas and experience stronger cultural noise. Recently, the Peterson low noise model was updated [10] by analyzing the absolute quietest data from the Global Seismographic Network (GSN). McNamara *et al.* presented the ambient noise levels from 159 worldwide broadband

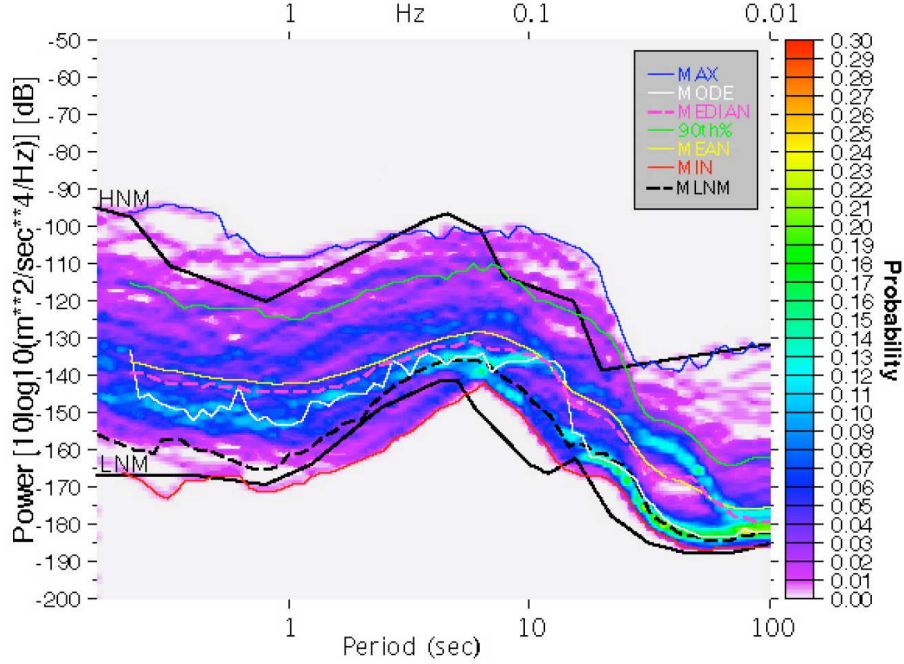


Figure 7: Power spectral densities of individual GSN and ANSS station modes used in McNamara's ambient seismic noise analysis [9].

seismic stations within the GSN and the Advanced National Seismic System (ANSS). For high frequencies (short periods) the minimum (corresponding to the red curve) is lower than the Peterson NLNM. However, the figure shows that this minimum has a low probability of occurrence (1 - 2%). For frequencies between 1 and 10 Hz, the minimum is dominated by station QSPA near the South Pole in Antarctica with its sensor at 300 m depth and is probably due to a spectral hole at 4 Hz due to the thick surface ice layer. Hence, it may not represent ambient noise conditions at the station.

2.3.1 Microseismic noise

Microseismic noise is a prominent feature for frequencies around 0.17 Hz and 0.07 Hz. The small low-frequency peak (periods of 10 - 16 s) correlates with the frequency of coastal waves, where the ocean wave energy is converted into seismic energy through either vertical pressure variations or from the surf crashing on shore. The large peak at about twice the frequency (periods of 4 - 8 s) originates from standing ocean waves that couple to the continental shelf. The standing waves are generated by superposition of ocean waves of equal period traveling in opposite directions and have recently been confirmed by satellite observations. Corresponding PSD values change up to 30 dB depending on the storm intensity, while the two frequencies shift upward as storms age. Fig. 8 shows PSD values at three locations. Station POHA is located in the center of the Pacific Ocean on Hawaii, SAO is less than 50 km from the coast of northern California and ISCO is located in a mine shaft in the mountains near Idaho Springs, Colorado. Microseismic activity is seen in all spectra. Note that also shifts in peak frequency can be observed.

It can be seen in Fig. 8 that there is a noise tail from the microseismic peak protruding into our frequency range of interest. This can be understood from modeling microseismic noise by a harmonic driver of frequency $f_0 = 0.17$ Hz whose phase suffers sudden changes at random time

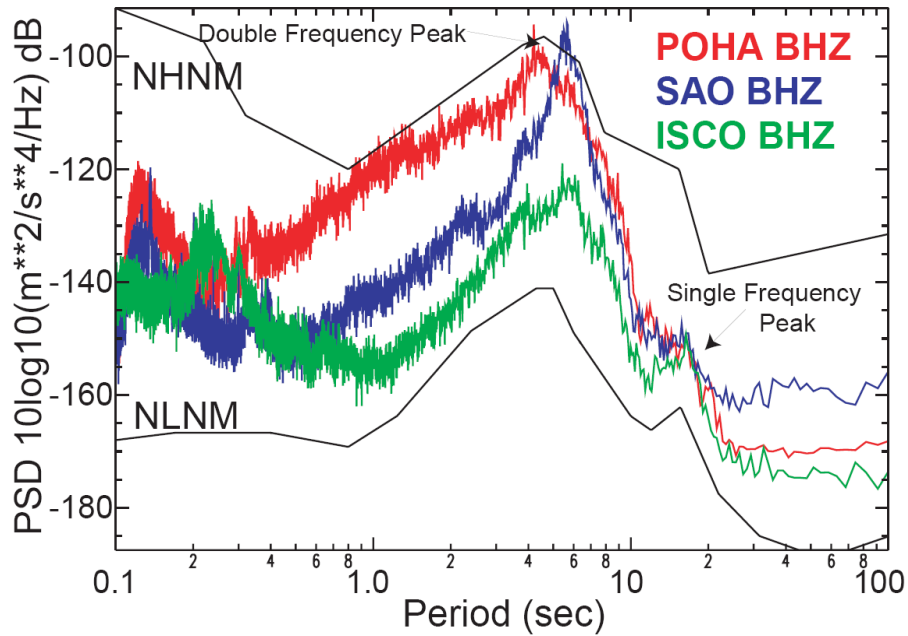


Figure 8: Microseismic noise at island, coastal and continental interior sites as measured on May 29, 2002 06:00:00 3600 seconds. Island of Hawaii, POHA BHZ (Red), Northern California, SAO BHZ (Blue), Continental interior, Colorado ISCO (Green). Note increasing microseismic noise from Colorado to California to Hawaii. [11].

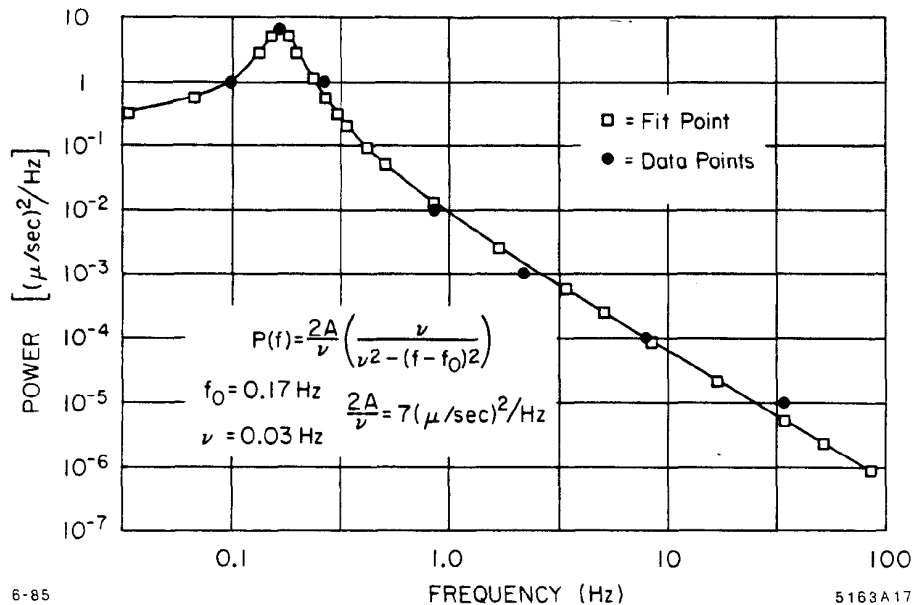


Figure 9: A fit by Fischer [12] to the long-term averaged maximum noise power spectra from [13].

intervals [12]. Fig. 9 shows that in this case the power density spectrum has the form

$$P(f) = \frac{2A}{\nu} \frac{\nu}{\nu^2 - (f - f_0)^2} \quad (3)$$

in units of power/unit frequency interval. The driver corresponds to the energy input of the standing ocean waves and microseisms is generated by Fourier components of random exciting fields that have the same phase velocities as free modes of the elastic system [14].

In the preliminary design of Einstein Telescope, the mirrors are separated by 10 km. Given a typical surface seismic wave speed of 400 m/s, the mirrors will experience a relative motion² for frequencies above about 0.02 Hz. It is concluded that at these low frequencies microseismic induced relative motion plays a role, and must be handled by the control systems of the test masses.

2.3.2 Cultural noise

The NLNM is a composite of different stations and instruments, with different geology and in various geographic regions. Therefore, it is not possible to duplicate its response at a specific location. It is observed that lowest noise is obtained in continental sites with sensors placed in hard rock. The sensors with lowest PSD values are borehole instruments operated at remote sites with low cultural noise. Lowest noise is obtained when there is no wind. In the USA the lowest noise sites are ANMO in New Mexico and Alaska.

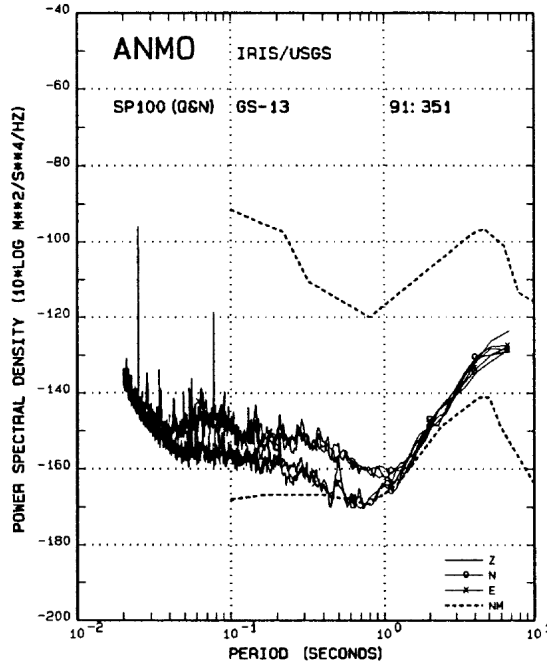


Figure 10: Noise spectra from the Albuquerque, New Mexico station for seismometers operated in the ASL subsurface vault [7].

ANMO is a borehole station of the Global Seismic Network (GSN) located in Albuquerque, New Mexico, USA. The sensor is located in granite at a depth of 100 m (at an elevation of 1740

²Note that here a $\lambda/2$ criterion has been applied.

m). Noise spectra from the ANMO subsurface vault are shown in Fig. 10. Around 1 Hz its lowest noise PSD is within 1 - 2 dB of the NLNM value, while for $1 < f < 10$ Hz two bands are visible due to cultural noise. Cultural noise mainly propagates as high frequency surface waves (1 - 10 Hz) that attenuate within several kilometers in distance and depth. Its signature can be seen in diurnal variations. The day-night spectral ratio for ANMO is shown in Fig. 11. Comparing median midday and midnight noise levels it is noted that cultural noise is visible at high frequencies. In the microseismic band (0.06 - 0.3 Hz) there are no day-night variations in excess of 1 dB at the ANMO site. Studies show [15] that in the frequency range 0.3 - 8.5 Hz the noise levels correlate over very large distances: the vertical-component up to 225 km, while horizontal component background noise correlates up to 175 km.

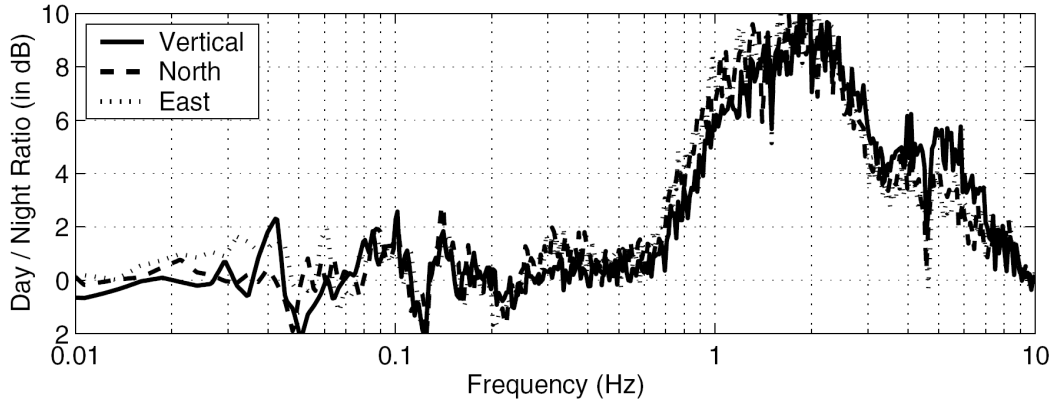


Figure 11: Midday versus midnight noise differences for the ANMO borehole station [15]. Cultural noise is visible for frequencies above 0.7 Hz.

While diurnal variations are limited to 10 dB above 1 Hz at the ANMO site, in more populated areas such as Binghamton, New York, the spectral ratios can be as high as 50 dB over long periods.

Spectrograms for frequencies up to 60 Hz have been made by Young *et al.* [27] with seismometers at the surface and within boreholes in the USA for data collected of more than one year. Seismometers were placed in boreholes at Amarillo, TX, at depths of 5, 100, 200, 367, 1219 and 1951 m. Cultural noise was present at all depths and most evident at 1219 and 1951 m (due to weaker wind-induced noise at these depths). Cultural noise exceeded background by about 10 dB and could be identified from diurnal patterns and was prominent for frequencies between 1 and 40 Hz. At Datil, NM, seismometers were installed at depths of 0, 5, 43, and 85 m and cultural noise was absent, most probably due to the remoteness of the site. At Pinedale, WY, with seismometers at depths of 3, 13, 30, 122 and 305 m, diurnal patterns in cultural noise were obscured by a pattern of progressive day-time increase of wind noise.

Traffic induced vibrations have been studied by various authors. Road noise depends on road structure and materials, traffic density and vehicle type and speed. McNamara & Buland [11] show that automobile traffic along a road only 20 m from station AHID in Auburn Hills, Idaho creates up to 35 dB increase in power in the 10 Hz frequency range. Lombaert and Degrange [21] carried out a study showing that the frequency spectrum broadens with increasing vehicle speed. Long [22] derived an empirical formula for attenuation of seismic road noise. It was found that where the intervening topology was greater than average (1 - 3 m), vibration levels decreased at 3 dB/m of relief. This was attributed by Long to surface waves scattering from the topography.

Schofield *et al.* [23] reported that local traffic, from passenger vehicles to heavy trucks, induced vibrations at the LIGO Hanford, WA, site. Vibrations were measured for frequencies in the 1 - 50 Hz range, with maxima around 4 - 12 Hz. Coward *et al.* [24] recorded ground vibrations at the AIGO site in Australia for vehicles passing the instrumentation as close as 24 m. Road noise was visible in the 5 - 30 Hz frequency band.

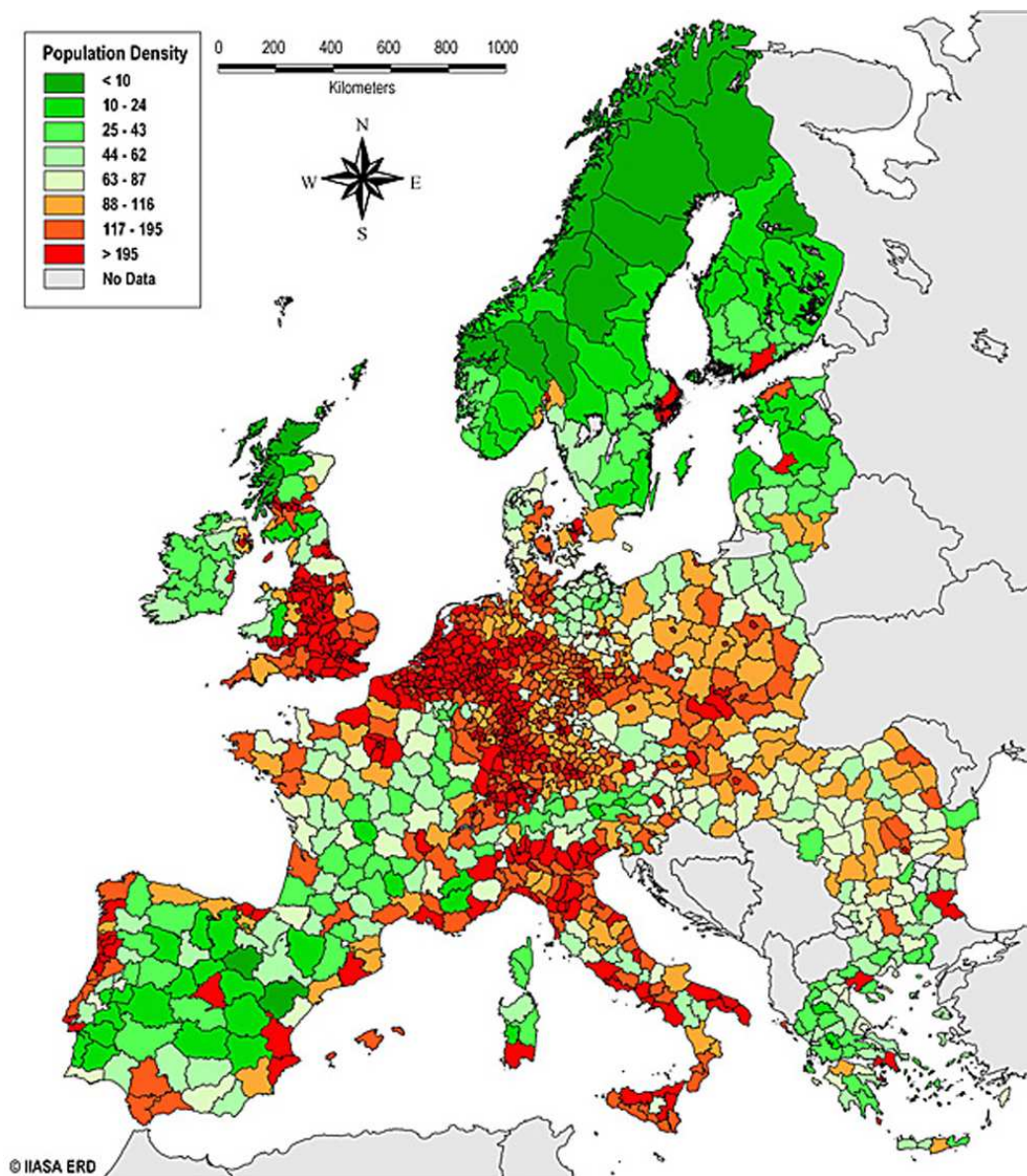


Figure 12: High frequency (1 - 10 Hz) seismic noise is driven by cultural noise. Density of population in Europe from the REGIO database of EUROSTAT [25].

Since cultural noise should strongly correlate with population density, we show in Fig. 12 an overview of the population density in Europe based on population data from the REGIO database of EUROSTAT.

2.3.3 Wind noise

Wind noise has been studied by a number of authors. Withers *et al.* [26] performed measurements at Datil, New Mexico. This is a remote site that features sparse vegetation. The nearest road is at 12 km distance and this road is lightly traveled. The distance to the nearest railroad is 90 km. Measurements were performed at a depth of 0, 5, 43 and 85 m. A reduction of 20 dB was found at a depth of 43 m. Young *et al.* [27] carried out measurements at Amarillo, Texas at a depth

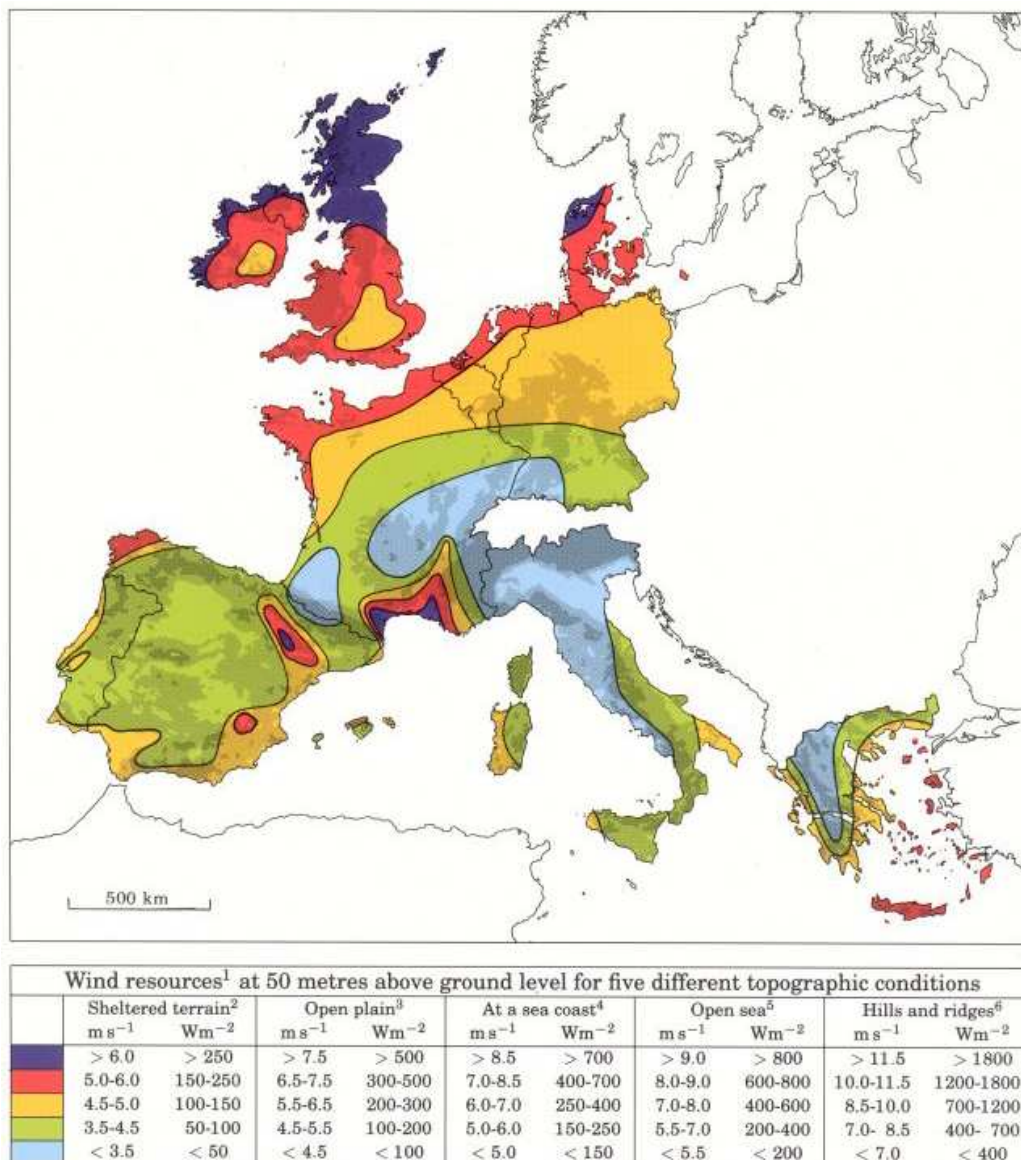


Figure 13: European wind resources based on data collected for the European Wind Atlas [28].

of 3, 13, 30, 122 and 305 m. A strong correlation between seismic noise and wind was observed over a broad frequency spectrum range from 1 to 60 Hz. The noise was 34 dB above the NLNM at at depth of 3 m, and decreased to 10 dB above NLNM at a depth of 305 m. In addition, it was observed that the wind speed threshold for inducing seismic noise depends on depth.

Fig. 13 shows an overview of the European wind resources based on the data collected for the

European Wind Atlas [28] and is based on comprehensive statistics from more than 200 stations covering the European Community.

2.4 Geological and geographic dependence

McNamara and Buland [11] have carried out a study of geographic dependence of ambient seismic noise in the USA. Fig. 14 shows that the strongest geographic dependence is obtained for

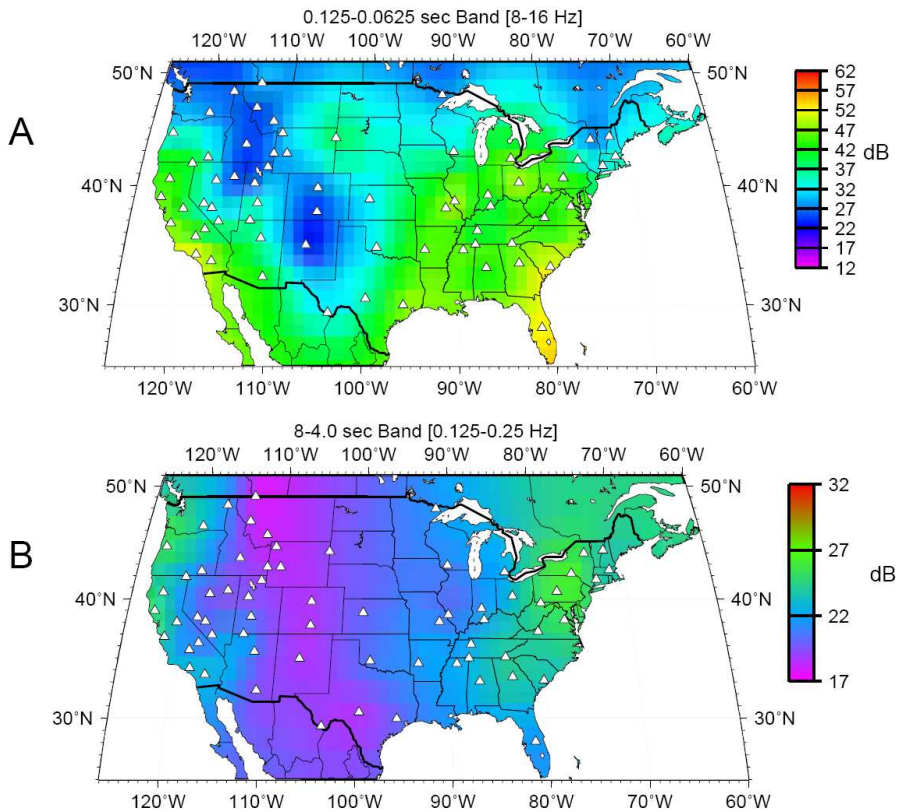


Figure 14: PSD noise levels above the NLNM mapped across the US in two separate frequency bands [11]: panel A or 8 - 16 Hz and panel B for 0.125 - 0.25 Hz.

frequencies above 1 Hz (panel A). Noise levels at the East coast are up to 50 dB above NLNM due to large population centers and represents cultural noise. Microseism shows up in the 0.125 - 0.25 Hz frequency range (panel B) and is dominant in coastal regions. The US continental interior has noise levels about 10 dB above NLNM.

Recently, OneGeology [29], an ambitious online project, under the direction of the British Geological Survey, started the collection of worldwide geological information. An example is shown in Fig. 15. Large areas of alluvium can be identified in Fig. 15. Alluvium is deposited soft soil composed of silt, clay, sand and gravel. Its material properties vastly differ from hard rock such as granite. This has immediate consequences for the ambient seismic noise levels as is demonstrated in Fig. 16. The seismic data shown in Fig. 16 have been obtained with the ORFEUS (Observatories and Research Facilities for European Seismology) network, a non-profit foundation that aims at coordinating and promoting digital, broadband seismology in the European-Mediterranean area. For frequencies around 2 Hz the seismic noise is almost 40 dB higher in alluvium (station GE.HLG) than hardrock (station CH.GIMEL). This is caused by the

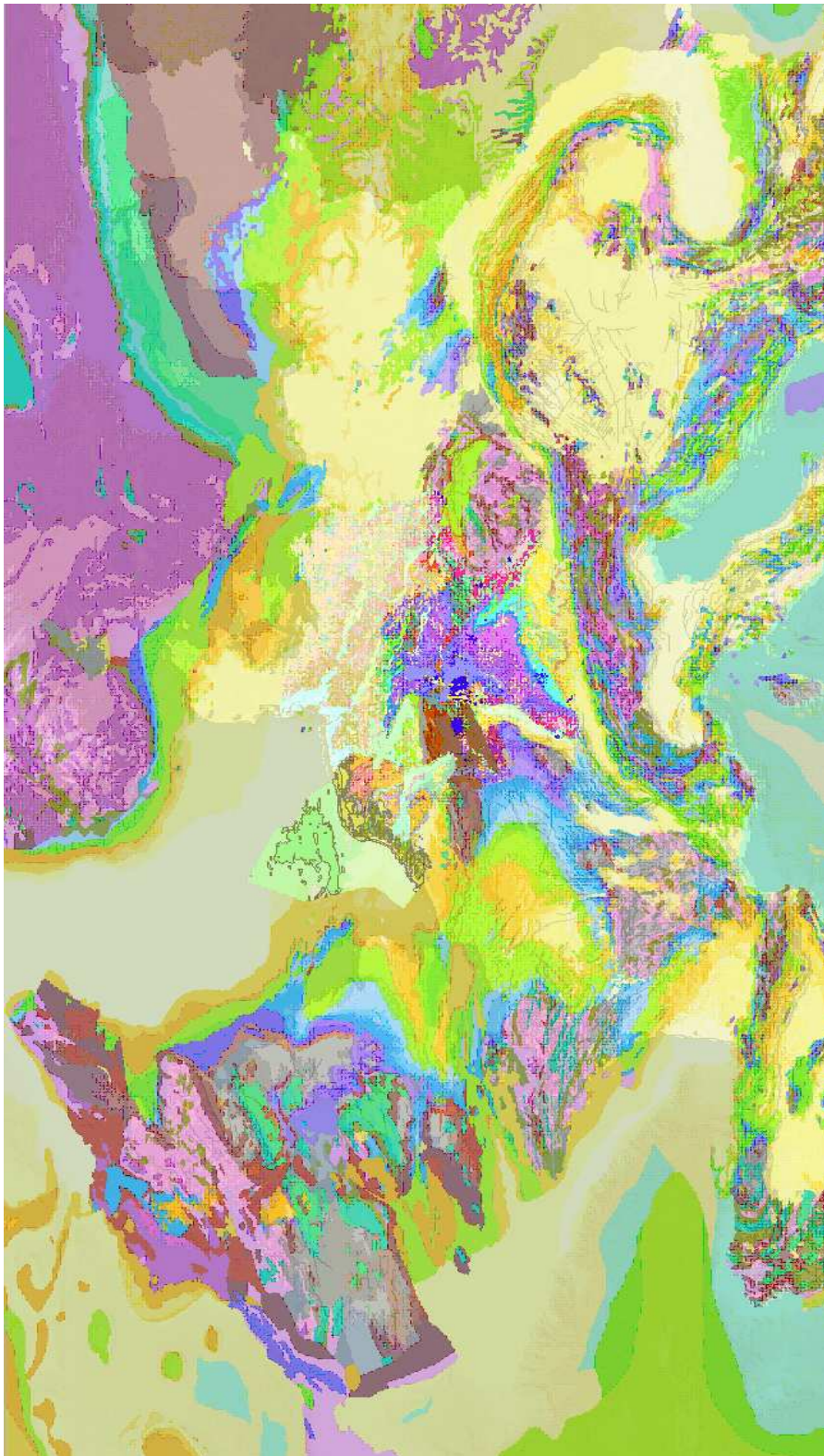


Figure 15: Geological map of Europe from the OneGeology portal [29]. The following geology is indicated: red corresponds to granite or basalt; pink - sandstone; green - chalk; purple - slate, limestone, mudstone; yellow - alluvium.

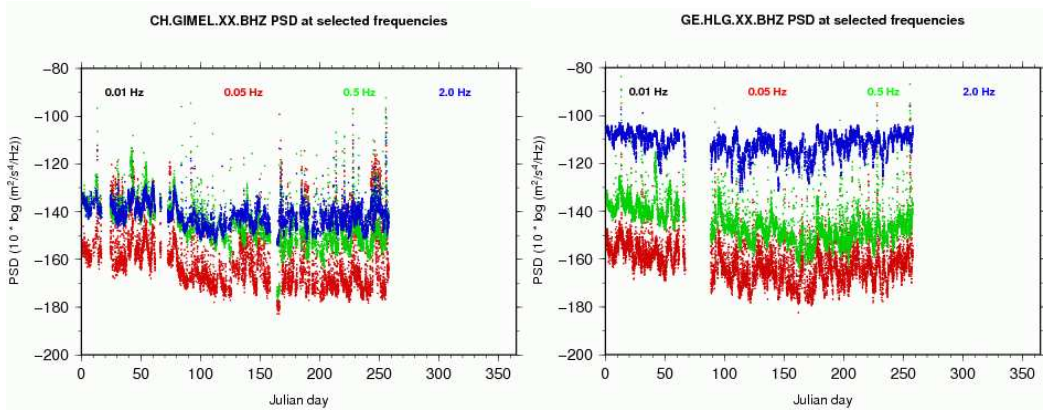


Figure 16: PSD noise levels obtained with the Orfeus network for station CH.GIMEL near Geneva, Switzerland and station GE.HLG near Hamburg, Germany. Data from reference [30].

lower velocity of seismic waves in sediments compared to hardrock. Areas dominated by alluvium can be found in the Netherlands, northern Germany and Poland, in the south of Germany, northern Italy (Po area), Toledo area in Spain, and eastern Europe. PSD values about 40 dB larger than hardrock have also been found in alluvium regions near Beijing, China and Santa Barbara, USA. Although for a surface site such regions should be avoided, this is at present not clear for an underground site.

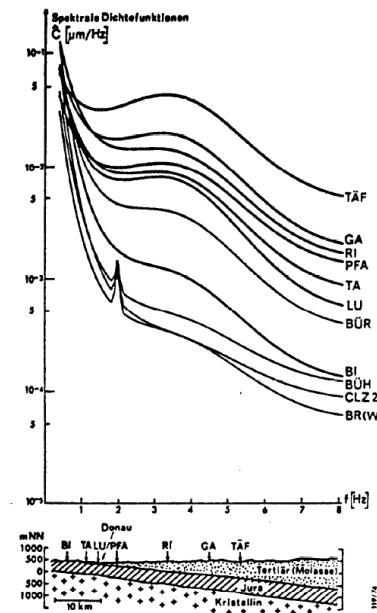


Figure 17: PSD ambient noise levels from a study for various locations in Germany [31].

Results of a systematic investigation of ambient noise in Germany [31] are presented in Fig. 17. Noise levels are lowest for sites in the south of Germany where geology is determined by crystalline granite formations. Highest ambient noise levels are recorded in the north of Germany where the hardrock layers are covered by alluvium (molasses). In between layers of harder Jura formations cover the crystalline granite. Average spectral densities are fitted with exponential

functions because of strong oscillations in PSD values. The signal at 2 Hz for the smallest spectral densities has been traced by a directional analysis to Rayleigh waves originating from the coast of Norway. The signal is believed to be due to choppy water waves in the shallow North Sea hitting the shore.

At first sight Scandinavia may be thought to provide suitable sites, since it is scarcely populated leading to low cultural noise, while the surface is dominated by old, good quality crystalline hardrock. However, seismic measurements from the KONO station near Kongsberg, Norway, show PSD values 20 - 30 dB above the NLNM (typically 140 dB around 1 Hz). It should be noted that the KONO sensor is located in a silver mine at 340 m depth. The ambient seismic noise is due to the high frequency tail from the microseismic peak. KONO data show that the microseismic peak shows large seasonal variations. Moreover, in the winter months additional seismic background noise can be expected from ice activity in the East Sea.

3 Specific sites

3.1 CLIO site at Kamioka, Japan

In Japan the Cryogenic Laser Interferometer Observatory (CLIO) is being commissioned in the Kamioka mine located 220 km west from Tokyo. CLIO is a locked Fabry-Perot interferometer and is a precursor of the ambitious Large Cryogenic Gravitational Telescope (LCGT), an underground cryogenic interferometer with 3 km long arms. Kamioka Mine of Mitsui Mining & Smelting Co., Ltd. is the largest lead-zinc mine in Japan and was composed of two mines, the Tochibora Mine and the Mozumi Mine, which had daily production rates of 5,200 and 1,800 metric tons of crude ore, respectively. In the mines, there are many massive pyro-metasomatic deposits which have been derived from the replacement of limestone. The deposits are composed of skarn minerals which mainly contain hedenberite. The country rock is generally hard and fine-grained stable bedrock (gneiss) with an elastic speed exceeding 6 km/s. Fig. 18 shows results from measurements at the Kamioka underground site (1000 m underground from the top of the mountain at an altitude of 358 m) along the Mozumi mining shaft. At 1 Hz the horizontal displacement noise is about $2 \text{ nm}/\sqrt{\text{Hz}}$. The spectrum at the CLIO site falls with f^{-2} and consequently at 10 Hz the noise reduces to about $20 \text{ pm}/\sqrt{\text{Hz}}$. (These data were at the limit of the sensitivity of the measurement instrument and represent an upper bound. Note that data obtained with an interferometric device are presented in Fig. (21) indicate lower ambient seismic noise.) Vertical displacement noise is about an order of magnitude larger at the surface, but is similar to the horizontal displacement noise at the location of the CLIO site. The data reveal an average reduction of seismic noise of about 10^2 (with 10^3 at 4 Hz) compared to the TAMA surface site, located in Mitaka city in the center of Tokyo. Moreover, since CLIO is situated on hardrock, Hida gneiss, it is expected that a significant fraction of seismic motion may be rejected as a common-mode contribution.

The quality of the site was tested with the 20 m LISM prototype interferometer and revealed long-term stable operation, mainly due to the low background noise and stable temperature. The underground environment was judged harmful for equipment, such as vacuum pumps and optics, because of the high humidity ($\approx 100 \%$). The humidity causes mold growth. Air dehumidifiers were in place, but induced too much vibration noise. For LCGT it is planned to supply dried air from a separate chamber. Measurements show that cryo-coolers based on pulse-tube refrigerators cause about 1 Hz vibrations (and high frequency sound) and that protection is needed. The interferometer control room suffers from heat deposition by electrical equipment

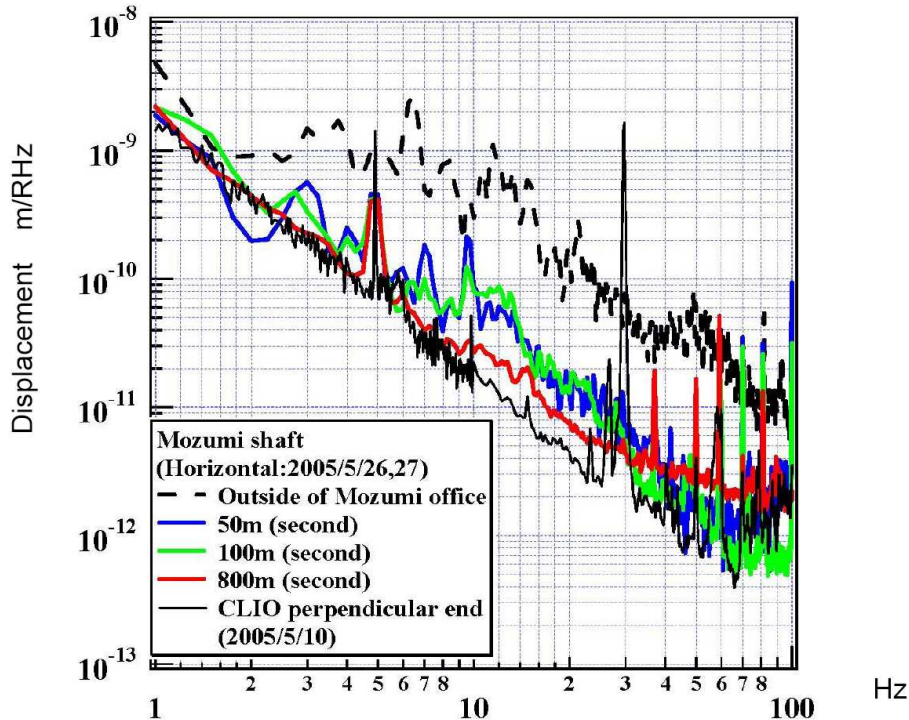


Figure 18: Horizontal displacement noise spectra of ambient seismic noise along the Mozumi mining shaft in Kamioka [32].

and human activity and requires a ventilation system. The optics suffer from dust contamination due to the mining history [32]. Dust in the (access) tunnels leads for example to a rapid degrading of laser power. A separate air lock for main chamber access is required. The horizontal access to the Kamioka facility is judged as very convenient. For LCGT clean, dry and cool air generation should occur far away from the interferometer. Air lock rooms should be realized between tunnels and laboratory areas, with walls between dusty arms and clean laboratory areas [36].

3.2 Homestake (Dusel) site at Black Hills, South Dakota, USA

The Deep Underground Science and Engineering Laboratory, Dusel is a project under consideration by the US National Science Foundation for the study of extremely rare nuclear physics processes. In July 2007 the NSF gave its approval to the Homestake Mine in South Dakota, USA as the future site for Dusel. The Homestake Mine is a deep underground gold mine (closed in 2002) located near Lead, South Dakota. It was the largest and deepest gold mine in North America, and is the site where solar neutrinos were observed first. When Dusel is realized with laboratories at 8,000 feet below ground, Homestake will be the deepest underground science facility. Presently (July 2009), the mine is flooded to about 5,000 feet depth.

Fig. 19 shows noise spectra from the RSSD station located in the Black Hills in South Dakota, USA. The origin of the step-like feature at low periods is unclear. The geology at the RSSD station is limestone and the sensor is placed in a borehole at a depth of 110 m and elevation of 1950 m. The figure shows that the PSD is about 15 dB above the NLNM around 1 Hz. These noise levels may be indicative for seismic noise at Homestake. Presently, a program is ongoing at Dusel to perform detailed seismic measurements [34]. A network of seismic sensors is being

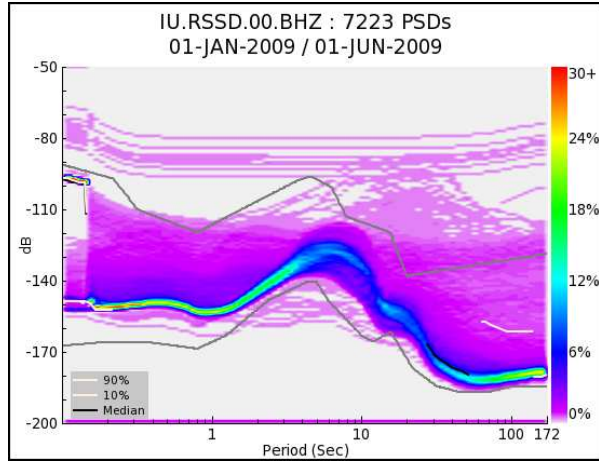


Figure 19: Power spectral density seismic noise data (2009) from the RSSD seismic station in the Black Hills, South Dakota, USA [33].

implemented that will collect data at various depths. Sensors are installed at 300, 800, 2000 and 4100 feet. Fig. (20) shows horizontal velocity densities measured at the Homestake site at a

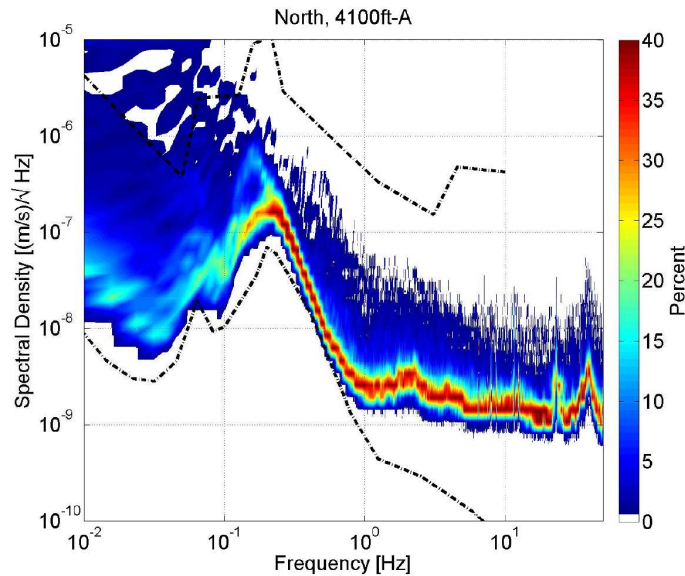


Figure 20: Horizontal velocity spectral density seismic noise data (2009) from a seismic station installed at the 4100 feet level at the Homestake site in Lead, South Dakota, USA [35].

depth of 4100 feet. The figure shows data for a two week period and was taken in summer 2009. The quiet-time spectra at 2000 feet depth are for low frequencies (< 0.5 Hz) close to NLNM. Time-averaged PSD spectra depend on microseisms and cultural noise and are typically about 10 dB above NLNM. The measured H/V ratio suggests that rock inhomogeneities are significant [35]. Strong coherence between the vertical signals from stations at 300 and 2000 feet is observed for frequencies around 0.2 Hz.

3.3 Sites in Germany

Displacement noise data have been analyzed [36] for the Black Forest Observatory, BFO, for the Seismologische Observatorium Berggieshübel, BRG, and for the Graefenberg, GRFO borehole station. The BFO station is realized in a formed nickel mine. The sensors are located at a depth of 162 m in granite base-rock, covered by sediments. BRG is an abandoned mine with hornblendeslates geology with sensors located at 36 m depth. GRFO is a 116 m deep borehole with sensors in chalk and dolomite. Fig. 21 shows quiet night-time horizontal displacement noise spectra for BFO, BRG and GRFO in comparison with data from Kamioka and GEO600. For reference also the SGN values from Ref. [10] are shown.

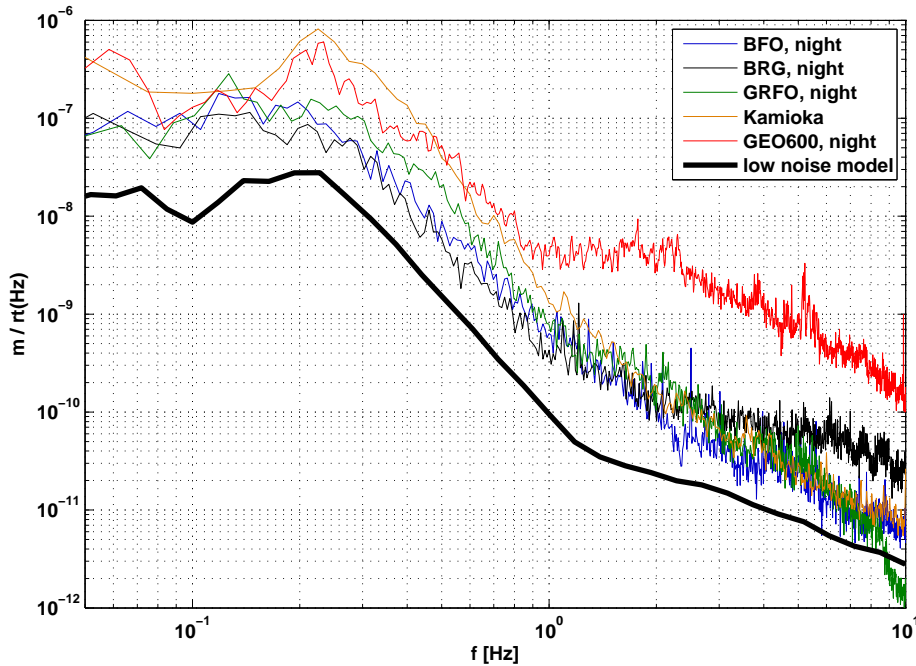


Figure 21: Displacement noise spectra from the BFO, BRG and GRFO seismic stations in Germany [36]. For comparison data from Kamioka and GEO600, and SGN [10] are shown.

The displacement noise of BFO, BRG and GRFO are comparable and amount to 0.5 - 0.8 nm/ $\sqrt{\text{Hz}}$ around 1 Hz and approximately drops as $1/f^2$ with frequency. Noise levels are less than an order of magnitude above NLNM and similar to the Kamioka values. Noise levels are significantly lower than those obtained at the GEO600 site. For BFO diurnal variations of about a factor 2 - 3 have been determined for frequencies in the range 1 - 10 Hz. Fig. 22 shows noise spectra from the BFO station located in the Black Forest in Germany. Anthropogenic noise is seen on working days, between 6 am and 4 pm. The noise is strongest around 5 Hz and is caused presumably by sawing mills in the vicinity of the site.

There are other sites in Germany that feature relatively low ($< 1 \text{ nm}/\sqrt{\text{Hz}}$) seismic noise. PSD values obtained at the Moxa seismic station near Jena and at a 900 m depth in the Asse rocksalt mine are below $1 \text{ nm}/\sqrt{\text{Hz}}$.

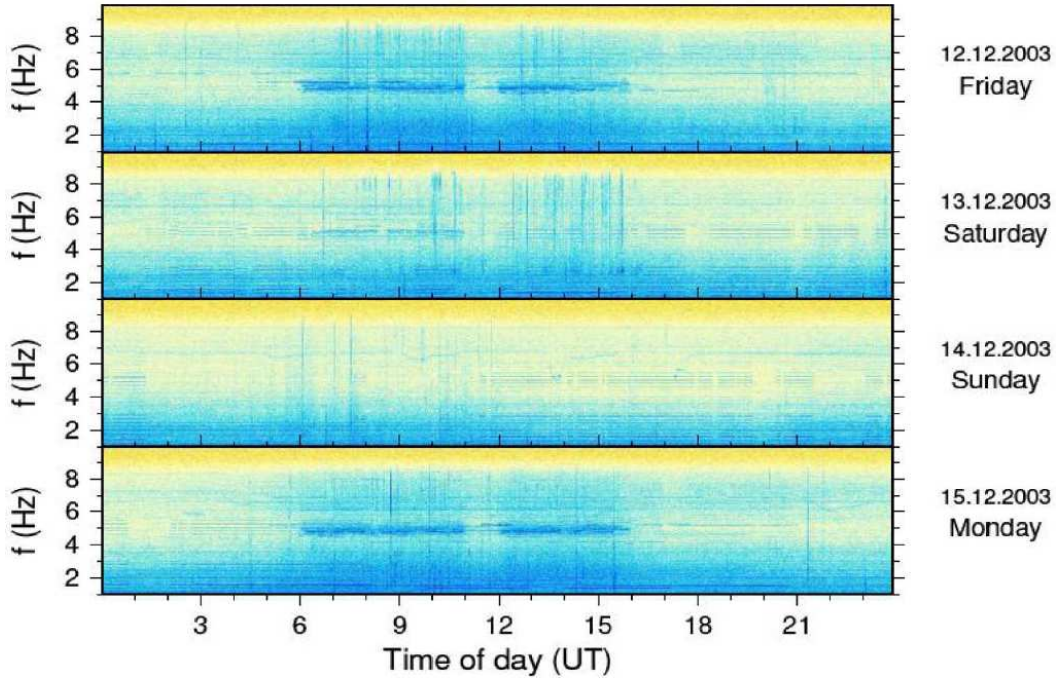


Figure 22: High frequency cultural noise at the Black Forest Observatory in Germany [37].

3.4 Experience from particle accelerator sites

Studies have been initiated to measure ground motion of various sites for characterization of the International Linear Collider (ILC) design. For the ILC vertical beamsizes in the order of 5 nm is needed to maintain collisions and to prevent emittance growth induced by betatron oscillations due to magnet movement. The site characterization program of DESY [38] consists of a comprehensive database of measured ground motion for various high energy laboratories, synchrotron light sources and reference sites. Fig. 23 (left panel) shows average PSD values

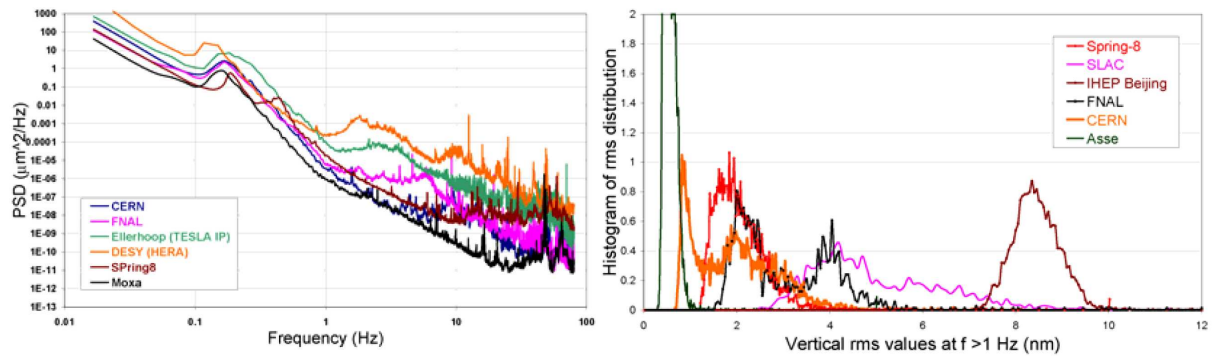


Figure 23: Left panel: average PSDs, in the vertical direction, of several sites, including the reference Moxa site; right panel: histogram of the rms distributions (at $f > 1$ Hz, in vertical direction) for 6 so-called quiet sites [38].

for the accelerator sites CERN LHC tunnel, Fermilab, DESY HERA tunnel, Spring8 and the considered interaction point (IP) of the Tesla collider. For reference the PSD of the Moxa seismic station near Jena is shown. In our frequency region of interest PSD values differ by 4 orders of

magnitude (3 orders of magnitude above Moxa at 1 Hz). The HERA ring at DESY is situated in a shallow tunnel in close proximity of the densely populated city of Hamburg. The geology of the area is dominated by alluvium: quaternary sand and marlstone. Lower PSD values are obtained for the CERN LHC tunnel. LHC is situated in a 100 m deep tunnel in stable bedrock. The rms vertical motion of the LHC tunnel is 1.8 nm at 1 Hz (compared to 0.6 nm rms for the Moxa site). The PSD spectra of the relatively deep LHC tunnel are about 3 orders of magnitude lower compared to the surface. A similar noise decrease with depth has been observed in measurements in the Numi tunnel (40 m depth) near Fermilab.

Fig. 23 (right panel) shows rms distributions for various sites that were judged to be quiet in the Desy site characterization studies [38]. For comparison, the results from measurements performed at a depth of 900 m in the Asse rocksalt mine is shown. Note that the CERN and Fermilab data show two peaks in their distribution attributed to diurnal effects. The Asse distribution has an average rms (at $f > 1$ Hz) of 0.5 nm and together with the Moxa site (rms of 0.6 nm) constitute the quietest sites of the study. Quiet sites include CERN LHC (rms 1.8 nm), FNAL (2.9 nm), IHEP Beijing (8.4 nm), SLAC (4.8 nm) and Spring-8 Harima (2 nm). Noisy sites include BNL (87.8 nm), DESY HERA (51.8 nm), ESRF Grenoble (71.6 nm), KEK Tsukuba (78 nm) and SSRF Shanghai (292 nm).

For accelerator design it is important to distinguish correlated motion from absolute motion. Coherence between synchronized seismometers has been measured at various sites. Measurements at DESY show that coherence is lost for frequencies above 1 Hz over distances of 600 m. Such information is site specific and can be used to model GGN subtraction and to determine the number of seismometers needed for such schemes.

It has been observed, especially at the noisy accelerator facilities that there are strong variations with time: day - night differences and differences between weekend and weekdays. However, also at quiet sites as SLAC in the USA, noise related to water pumps, water in cooling pipes and cryogenic fluids was identified. Low frequency reciprocating devices often generate well defined sharp spectral lines. These devices include vacuum pumps, and compressors using air, helium or hydrogen. To handle such laboratory generated noise a strict site policy should be developed and implemented, since later mitigation can be costly.

4 Site requirements from logistical arguments

It is paramount to identify the criteria for site selection and evaluation at an early stage [39]. The selected site should allow the highest possible level of scientific productivity at reasonable cost of construction and operation, and at minimal risk. Of paramount importance are the selection criteria that impact the scientific potential of Einstein Telescope. These include natural and man-made ground vibrations and site geological constraints that affect critical parameters as interferometer arm lengths. This report has focused on these issues

Site requirements that impact construction cost must be considered. These include topography and geological subsurface conditions. Factors such as horizontal versus vertical access to the underground facilities greatly affect the construction costs. Site availability and acquisition costs can vary greatly. Availability of existing support infrastructure is important. Underground laboratories as Laboratori Nazionali del Gran Sasso LNGS (Italy), Laboratoire souterrain de Modane LSM (France), Laboratorio Subterráneo de Canfranc LSC (Spain), and Institute for Underground Science, Boulby Mine (UK) provide extensive facilities for scientific and technical staff. This includes accommodations for resident staff (housing, schools, etc.), and visiting staff

(lodging, transportation, etc.). For the same reason active or closed-down mines may provide valuable facilities such as hosting shafts, electrical infrastructure, water pumps, and safety systems. In addition, they may provide local technical support and experienced technical staff. Other factors that determine the (cost of) the main infrastructure design include groundwater conditions, hydrology and drainage which have an impact on the design of buildings and tunnels, accessibility such as roads, railroad, distance to nearby supporting technical facilities, site utilities installations as power, water, and sewage. Finally, labor costs and proximity of soil waste and borrow areas must be considered.

Various factors impact the operation cost. These include the cost of electrical power, cost of local labor, heating and cooling requirements, maintenance requirements, and travel time and cost for visiting staff. Environmental, health and safety plans must be put in place to assure the safety of users, staff, and visitors to Einstein Telescope. These plans must comply with relevant governmental standards and regulations. It is important to elevate the life-safety level above that in the mining and underground construction industries to one appropriate for researchers, students, and the public.

Risks must be minimized in the realization of Einstein Telescope. Risk factors include acquisition risk, risks from environmental sources such as earthquakes, floods and storms. Special attention must be paid to potential future man-made noise and vibration from development or industrial projects.

5 Summary

Various selection criteria for candidate sites for Einstein Telescope have been discussed. Special attention has been paid to seismic noise since this has the greatest impact on the scientific capabilities. It has been shown that the seismic displacement noise that affects the performance of the observatory most, is driven by ocean, wind and human activity (*e.g.* logging, cars, and heavy machinery). Consequently, it is imperative to carry out a careful site selection where candidate sites must be explored in detail. Such studies will be performed in collaboration with European geosciences groups, as the Italian National Institute for Geophysics and Volcanology. The use of active control systems with feedback of information from seismometers, accelerometers, strainmeters, tiltmeters, rock thermometers and piezometers to the test masses will be investigated.

Results from the above described studies will be used to identify a possible R&D path to gravity gradient correction systems. Simulations to study type and number of sensors, sensor network configuration and noise subtraction procedures must be carried out.

Acknowledgements

This work has been performed with the support of the European Commission under the Framework Programme 7 (FP7) Capacities, project Einstein Telescope design study (Grant Agreement 211743), <http://www.et-gw.eu/>. This work is part of the research programme of the Foundation for Fundamental Research on Matter (FOM), which is financially supported by the Netherlands Organisation for Scientific Research (NWO). We gratefully acknowledge the support of LIGO

References

- [1] ET - WG3 report, *Pushing towards the ET sensitivity using 'conventional' technology*, S. Hild, S. Chelkowski and A. Freise, arXiv:0810.0604v2 (November 2008).
- [2] B.A. Baklakov *et al.*, *Investigation of Correlation and Power Characteristics of Earth Surface Motion in the UNK Complex Region*, Preprint INP 91-15, Novosibirsk (1991); see the same authors in Proc. of 1991 IEEE Particle Accel. Conf., San-Francisco (1991); *Study of Seismic Vibrations for the VLEPP Linear Collider*, Tech. Phys., v.38, p.894 (1993), Zh. Tech. Fiz., v.63, No.10, p.122 (1993).
- [3] V. Parkhomchuk and V. Shiltsev, *Fractal Model of Ground*, Preprint INP 92-31, Novosibirsk (1992, in Russian), and Proc. of Int. Workshop on Linear Colliders, Garmish-Partenkirchen, Germany (1992).
- [4] *Space-Time Ground Diffusion: The ATL Law for Accelerators*, V. Shiltsev, Proceedings of the 4th International Workshop on Accelerator Alignment (IWAA 1995) 14-17 November 1995, Tsukuba, Japan.
- [5] V. Parkhomchuk *et al.*, *Slow Ground Motion and Operation of Large Colliders*, Particle Accelerators, vol. 46, No. 4, pp.241-258 (1994), and SSCL-Preprint-470 (1993).
- [6] Bundesanstalt für Geowissenschaften und Rohstoffe (BGR), Hannover, Germany (<http://www.bgr.bund.de/>).
- [7] *Observations and modeling of seismic background noise*, J. Peterson, Open-File report 93-322, U.S. Department of Interior Geological Survey (1993).
- [8] *Preliminary observations of noise spectra at the SRO and ASRO stations.*, J. Peterson, Open-File report 80-992, Washington, DC: U.S. Geological Survey (1980).
- [9] *Ambient seismic noise*, D.E. McNamara *et al.*, USGS report, (August 2005).
- [10] *Ambient Earth noise: a survey of the global seismographic network.*, J. Berger *et al.*, J. Geophys. Res., 109 (2005).
- [11] McNamara, D. E. and R.P. Buland, *Ambient Noise Levels in the Continental United States*, Bull. Seism. Soc. Am., 94, 4, 1517-1527, 2004.
- [12] G.E. Fischer, *Ground motion and its effects in accelerator design*, SLAC - PUB - 3392 REV (July 1985).
- [13] *Quantitative Seismology*, Vol. I, K. Aki and P. Richards, Freeman & Co., 1980.
- [14] *A Statistical Analysis of the Generation of Microseisms*, K. Hasselman, Reviews of Geophysics, Vol. 1, May 1963.
- [15] *Broadband Seismic Background Noise at Temporary Seismic Stations Observed on a Regional Scale in the Southwestern United States*, D. Wilson *et al.*, Bulletin of the Seismological Society of America, Vol. 92, No. 8, pp. 3335 - 3341 (December 2002).
- [16] *Gebirgsmechanische Zustandsanalyse des Tragsystems der Schachanlage Asse II*, Kurzbericht. Institut für Gebirgsmechanik GmbH, Leipzig, 2007.

- [17] *SESAME: Site effects assessment using ambient excitations. Final report, WP08, Nature of noise wavefield.* European Commission. <http://sesame-fp5.obs.ujf-grenoble.fr/>, P-Y. Bard *et al.* (2003).
- [18] *Microseisms*, B. Gutenberg, *Advances in Geophysics* 5: 53 - 92 (1958).
- [19] *Geological-control of the three-component spectra of Rayleigh-wave microseisms*, M.W. Asten, *Bulletin of the Seismological Society of America* 68, 1623 - 1636 (1978); *Arrays estimators and the use of microseisms for reconnaissance of sedimentary basins*, M.W. Asten and J.D. Henstridge, *Geophysics* 49: 1828 - 1837 (1984).
- [20] *Overview of Seismic Noise and its Relevance to Personnel Detection*, L. Peck, ERDC/CRREL TR-08-5, Us Army Corps of Engineers, Engineer Research and Development Center (April 2008).
- [21] Lombaert, G., and G. Degrande. *Experimental validation of a numerical prediction model for free field traffic induced vibrations by in situ experiments.* *Soil Dynamics and Earthquake Engineering* 21: 485 - 497 (2001); Lombaert, G., G. Degrande, and D. Clouteau. *Numerical modeling of free field traffic-induced vibrations.* *Soil Dynamics and Earthquake Engineering* 19: 473-488 (2000).
- [22] Long, L.T. 1993. *Measurements of seismic road vibrations.* In *Proceedings of the Third International Conference on Case Histories in Geotechnical Engineering*, Paper 4.10, p. 677-680 (1993).
- [23] Schofield, R., M. Ito, E. Mauceli, H. Radkins, C. Gray, G. Moreno, and G. Gonzalez. *Source and propagation of the predominant 1-50 Hz seismic signal from off-site at LIGO-Hanford.* LIGO Scientific Collaboration Meeting, LIGO Hanford Observatory, Hanford, Washington, 15-17 August 2000. See also http://admdbsrv.ligo.cltech.edu/meetings/lsc_default.htf?meetingid=6.
- [24] Coward, D., D. Blair, R. Burman, and C. Zhao. *Vehicle-induced seismic effects at a gravitational wave observatory.* *Review of Scientific Instruments* 74: 4846 - 4854 (2003).
- [25] European Commission Joint Research Center. See <http://ec.europa.eu/dgs/jrc/index.cfm>
- [26] *High-frequency analysis of seismic background noise as a function of wind speed and shallow depth*, M.M. Withers *et al.*, *Bulletin of the Seismological Society of America* 86: 1507 - 1515 (1996).
- [27] *A comparison of the high-frequency (>1 Hz) surface and subsurface noise environment at three sites in the United States*, C.J. Young *et al.*, *Bulletin of the Seismological Society of America* 86: 1516 - 1528 (1996).
- [28] See <http://www.windatlas.dk>.
- [29] See <http://www.onegeology.org/>.
- [30] See <http://www.orfeus-eu.org/>.
- [31] M.Steinwachs, *Systematische Untersuchung der kurzperiodischen seismischen Boderumruhe in der Bundesrepublik Deutschland*, *Geologisches Jahrbuch, Reihe E, (Geophysik) E3* Hannover (1974).
- [32] K. Kuroda, private communications (2009).

- [33] See <http://earthquake.usgs.gov/research/monitoring/operations/>.
- [34] V. Mandic, private communications (2009).
- [35] J. Harms, Underground seismic measurements, first steps at Homestake, GWADW, Ft. Lauderdale, Florida, USA (May 2009).
- [36] H. Grote, Seismic Data from the Black Forest Underground Station and Experience from Kamioka, ET - WP1 meeting, Gran Sasso, (Feb. 2009).
- [37] Black Forest Observatory (BFO). See <http://www-gpi.physik.uni-karlsruhe.de/pub/widmer/BFO/>.
- [38] R. Amirikas, A. Bertolini, W. Bialowons, H. Ehrlichmann, *Ground Motion and Comparison of Various Sites*, Proceedings of NANOBEAM2005, 36th ICFA Advanced Beam Dynamics Workshop, Editors: Y. Honda, T. Tauchi, J. Urakawa (KEK), Y. Iwashita and A. Noda (Kyoto), pages 202-206, <http://atfweb.kek.jp/nanobeam/files/proc//proc-WG2b-01.pdf> and EUROTeV Report 2005-023-1, http://www.eurotev.org/reportspresentations/eurotevreports/2005/index_eng.html; See also <http://vibration.desy.de>.
- [39] The procedures developed for the site selection of LIGO, Virgo and accelerator projects provide an important source of information.